Numerical Simulation Method of radiation damage effects in plate-type dispersion nuclear fuel elements

Yunmei Zhao, Shurong Ding*, Xin Gong, Yongzhong Huo
Department of Mechanics and Engineering Science, Fudan University, Shanghai 200433, China
* Corresponding author: dsr1971@163.com

Abstract A metal-matrix dispersion nuclear fuel plate is composed of dispersion nuclear fuel meat and metal cladding. The fuel meat is similar to a kind of particle composite with the fuel particles embedded in the metal matrix. The extremely harsh irradiation environment results in the complex thermo-mechanical coupling behaviors occurring in the dispersion fuel plate. Especially, this complexity stems more from the irradiation damage effects, such as irradiation hardening and creep in the metal materials induced by the high-energy fission fragments and neutrons, and the thermal conductivity degradation of fuel particles as well. In this study, for heterogeneous irradiation conditions, the three-dimensional large deformation constitutive relations and stress update algorithms are built and validated for the homogenized fuel meat and cladding in the co-rotational coordinate system through forming subroutines in ABAQUS. The obtained results for the whole fuel plate indicate that when the non-homogeneous irradiation condition introduced: (1) both the mechanical and temperature fields show remarkable non-uniform characters along the length direction; (2) the deformation of the plate surface tends to be an arch, which could affect the normal flow of coolant with increasing burnup. The developed numerical simulation method provides a convenient way to simulate the heterogeneous irradiation damage. This study can lay a basis for establishing failure criteria for metal materials in the irradiation environment.

Keywords radiation damage, stress update algorithm, non-homogeneous irradiation condition, thermo-mechanical coupling

1. Introduction

Dispersion nuclear fuel elements are composed of metal cladding and fuel meat [1] with a certain volume fraction of fuel particles embedded in the matrix. Compared to the presently used nuclear fuel elements in nuclear plants, they have much better thermal conductivity and thus can reach higher burnup. They have a promising usage in the advanced nuclear reactors and disposal of nuclear wastes. The thermo-mechanical behaviors evolution of nuclear fuel elements and assembly is one of the mostly concerned issues for their in-pile safety, and it is a critical issue in their optimal design as well. Recent researches on thermo-mechanical behaviors in dispersion fuel elements with the finite element method (FEM) have been becoming a development trend, and the numerical simulation method is expected to be an important way for their optimal design. Some finite element method codes, such as FASTDART [2-3], PLATE [4-5], MAIA [6-7] and DART-TM [8], were developed with the attempt to study their thermal and thermal-mechanical behaviors. Van Duyn's study [9] treated the rod-like dispersion fuel pellet as a composite and established a three-dimensional model with the mutual interaction between the particles and matrix considered. Shurong Ding [10-11]studied the thermal and mechanical behaviors and Qiming Wang [12] studied the interfacial behaviors of the plate-type dispersion nuclear fuel elements based on the Representative Volume Element (RVE) method. In the demanding environment of nuclear reactors,

irradiation swelling occurs in nuclear fuels, and their thermal conductivity is degraded due to nuclear fissions; the metal materials within fuel elements experience irradiation damage effects, such as irradiation hardening and creep [13]. Besides, for the dispersion nuclear fuel plate, the research of nuclear reactor physics indicates that the irradiation damage along the length direction is heterogeneous owing to the non-homogeneous distribution of fast neutrons. All the above researches haven't well taken the irradiation damage effects into account, and a good simulation method for un-uniform irradiation conditions is waiting to be developed.

In order to study the thermo-mechanical behaviors of a whole fuel plate under non-homogeneous irradiation conditions, in this study, based on micromechanics, an equivalent fuel meat is obtained with the homogenized thermo-mechanical material properties related to the ones of fuel particles and metal matrix. With the thermo-elastic and irradiation swelling effects in the equivalent fuel meat, and with the thermo-elasto-plastic and irradiation hardening behaviors involved in the metal cladding, the respective three-dimensional thermo-mechanical constitutive relations and stress update methods are constructed. Assuming that the heat generation rates and neutron flux along the plate length direction are linear with the maximums appearing in the middle location, the numerical simulation methods are realized through several subroutines in ABAQUS. The material points have been given different constitutive relations according to time and their locations, thus the time and location-dependent constitutive relation can be carried out. The proposed numerical method is validated and the un-uniform thermo-mechanical fields are obtained and analyzed.

2. The constitutive relations and numerical simulation methods

The whole fuel plate is regarded as the research object in this study and its thermo-mechanical behaviors evolution is focused on under the heterogeneous irradiation conditions. In the fuel meat, there contain a large number of fuel particles. It is impossible to consider the mutual interactions between the fuel particles and the matrix in the finite element model and it is necessary to deal with it as an equivalent homogenous material. As follows, the equivalent thermo-mechanical parameters are obtained on the base of homogenization theory. Owing to the temperature-dependent and time-dependent performances of the component materials together with the resultant location-dependent ones due to the heterogeneous irradiation conditions, the equivalent meat also has the above special properties. For the fuel cladding, the irradiation hardening effect is included in the large-deformation thermo-elasto-plastic behaviors.

For the fuel meat and cladding, the thermal constitutive relations are comparably simple, which can be implemented with the subroutine UMATHT. According to the temperature, location and real time of the incremental step, the integration points can be applied with different thermal constitutive relations. In the following, the mechanical constitutive relations are mainly built and the relative numerical simulation methods are given.

2.1. Constitutive models of the equivalent fuel meat

2.1.1. Parameters of the equivalent meat

Homogenization theory [14-15] has been introduced to a dispersion nuclear fuel meat, and the

material properties including both the mechanical and thermal properties are obtained as follows.
According to the mean field model by MAXWELL [16], the conductivity of the equivalent meat $\mathrm{K(T,t,X)}$ can be described as:

$$\mathrm{K(T,t,X)} = \frac{K_m(2K_m+K_p-2V_f(K_m+K_p))}{2K_m+K_p+V_f(K_m-K_p)}, \tag{1}$$

Where K_m and K_p separately represent the conductivity of the matrix and the inclusion phase of fuel particles.
This analysis adopts Mori-Tanaka Method [17] to calculate the equivalent Young's modulus and Poisson's ratio. That's:

$$\mathrm{E(T,t,X)} = E_m(1+\frac{V_f(\frac{E_p}{E_m}-1)}{1+(1-V_f(E_p/E_m-1)}; \upsilon = \upsilon_m(1+\frac{V_f(\frac{\upsilon_p}{\upsilon_m}-1)}{1+(1-V_f(\upsilon_p/\upsilon_m-1)}, \tag{2}$$

where E is equivalent Young's modulus (MPa) and υ is the equivalent Poisson's ratio, they are related to the Young's Modula and Poisson's ratios of fuel particles and matrix.
Only the fuel particles in the dispersion fuel meat can generate heat, and the heat generation rate of the particles corresponds to their fission rate. The heat generation rate of the fuel particles $\dot{q_p}$ can be expressed as

$$\dot{q_p}(X) = c \cdot \dot{f}, \tag{3}$$

with the unit is W/mm^3. Where $\mathrm{c} = 3.204 \times 10^{-11}$J/fission is the generated heat energy every fission event and $\dot{f}$ is the fission rate of fuel particles, while in this analysis the value of $\dot{f}$ is linearly distributed along the length direction like the fast neutrons, which has the largest one $0.6408\ \mathrm{W}/mm^3$ in the middle location as twice as the lowest one at the margin of the fuel meat.
The corresponding heat generation rate of the equivalent meat can be obtained as:

$$\dot{q(X)} = V_f \cdot \dot{q_p} \tag{4}$$

The swelling rate of the equivalent meat is obtained similarly as

$$\mathrm{SW(T,t,X)} = \frac{\Delta \mathrm{V}}{\mathrm{V_0}} = V_f \cdot \mathrm{SW}_p, \tag{5}$$

where $\dot{q_p}$ and SW_p separately denote the heat generation rate and swelling rate of fuel particles, they are both location-dependent and SW_p increases with burnup [3].
The thermal expansion of the equivalent meat α_c can be expressed as

$$\alpha_c(T) = 5.84 \times 10^{-6} + 1.9 \times 10^{-7} \times \frac{V_f-0.1}{0.05} + 2 \times 10^{-7} \times \frac{T-350}{450}, \tag{6}$$

where T is temperature in Kelvin with the application range from 350K to 730K.
In the above equations, the subscript p represents the material parameters of the fuel particles and subscript m represents the ones of matrix, and V_f denotes the volume fraction of fuel particles in the fuel meat. In this study, the considered volume fraction is 10%. Under heterogeneous irradiation conditions, the above obtained equivalent parameters vary with location, temperature and time.

2.1.2. Constitutive relationship of the equivalent meat

The large-deformation elastic constitutive relationship for the equivalent meat in a co-rotational coordinate system can be expressed as the following relation between Cauchy stress and elastic logarithmic strain:

$$\sigma_{ij} = \lambda(T,t,X)\delta_{ij}{\varepsilon_{kk}}^{el} + 2\mu(T,t,X){\varepsilon_{ij}}^{el}, \tag{7}$$

where $\lambda(T,t,X)$ and $\mu(T,t,X)$ is the Lame constants, they are related to the Young's Modulus and Poisson's ratio in Eq. (2).

The incremental form for a time step from t to $t+\Delta t$ with the temperature change from T to T+ΔT in a corotational framework can be obtained as

$$\Delta\sigma_{ij} = \lambda(T+\Delta T, t+\Delta t, X)\Delta\varepsilon_{kk}^{el}\delta_{ij} + 2\mu(T+\Delta T, t+\Delta t, X)\Delta\varepsilon_{ij}^{el} + \Delta\lambda\varepsilon_{kk}^{el(t)}\delta_{ij} + 2\Delta\mu\varepsilon_{ij}^{el(t)} \quad (8)$$

$$\Delta\varepsilon_{ij}^{el} = \Delta\varepsilon_{ij} - \Delta\varepsilon_{ij}^{th} - \Delta\varepsilon_{ij}^{sw} \quad (9)$$

$$\Delta\lambda = \lambda(T+\Delta T, t+\Delta t, X) - \lambda(T, t, X), \Delta\mu = \mu(T+\Delta T, t+\Delta t, X) - \mu(T, t, X) \quad (10)$$

where $\Delta\varepsilon_{ij}$ represents the total strain increment and $\Delta\varepsilon_{ij}^{el}$ represents the elastic one, $\varepsilon_{ij}^{el(t)}$ depicts the elastic strain at time *t*; $\Delta\varepsilon_{ij}^{th}$ and $\Delta\varepsilon_{ij}^{sw}$ mean the thermal strain increment and swelling one as the following

$$\Delta\varepsilon_{ij}^{th} = (\ln(1+\alpha_{c(T+\Delta T)}(T+\Delta T-T_0) - \ln(1+\alpha_{c(T)}(T-T_0))\delta_{ij} \quad (11)$$

$$\Delta\varepsilon_{ij}^{sw} = \frac{1}{3}\delta_{ij}(\ln(1+\mathrm{SW}(\mathrm{T}+\Delta\mathrm{T}, \mathrm{t}+\Delta\mathrm{t}, \mathrm{X})) - \ln(1+\mathrm{SW}(\mathrm{T}, \mathrm{t}, \mathrm{X}))) \quad (12)$$

Where T_0 is the reference temperature which is set as 350K.

2.2. Constitutive relationship of the cladding

2.2.1. Irradiation hardening model for the cladding material

The strain-hardening curve of unirradiated Zircaloy is described as [18]

$$\sigma = \mathrm{K}\varepsilon^n \cdot (\frac{\dot{\varepsilon}}{10^{-3}})^m \quad (13)$$

where σ is the true stress(Pa), ε is the true strain, n is the strain-hardening exponent, *K* is the strength coefficient and *m* is the strain rate sensitivity exponent. $\dot{\varepsilon}$ is the true strain rate. If $\dot{\varepsilon} < 10^{-5}/s$, set $\dot{\varepsilon} = 10^{-5}/s$.

$$\mathrm{K} = 1.17628\times10^9 + T(4.54859\times10^5 + T(-3.28185\times10^3 + 1.72752T)) \quad (14)$$

$$\mathrm{n} = -9.49\times10^{-2} + T(1.165\times10^{-3} + T(-1.992\times10^{-6} + 9.588\times10^{-10}T)) \quad (15)$$

$$\mathrm{m} = 0.02 \quad (16)$$

where *T* is the temperature in Kelvin ranged from 300 K to 730K.

Due to the irradiation hardening effect, the strain hardening exponent [18] is described by further multiplying the coefficient given in Eq. (17)

$$k_2 = 1.369 + 0.032\times10^{-25}\cdot(\phi\cdot t) \quad (17)$$

The strength coefficient under irradiation [18] is given by adding the value given in Eq. (14) to Eq.(18)

$$k_3 = 5.54\times10^{-18}\cdot(\phi\cdot t) \quad (18)$$

The factors in Eqs. (17-18) are both dimensionless, and $\phi\cdot t$ denotes the fast neutron fluence (n/m^2); $\phi$is the fast neutron flux, which is location-dependent due to the heterogeneous irradiation conditions.

2.2.2. Three-dimensional constitutive relation for the cladding

The incremental constitutive relation for the cladding is similar to Eq. (8) as

$$\Delta\sigma_{ij} = \lambda(T+\Delta T, t+\Delta t, X)\Delta\varepsilon_{kk}^{el}\delta_{ij} + 2\mu(T+\Delta T, t+\Delta t, X)\Delta\varepsilon_{ij}^{el} + \Delta\lambda\varepsilon_{kk}^{el(t)}\delta_{ij} + 2\Delta\mu\varepsilon_{ij}^{el(t)}$$

Since the large-deformation thermo-elasto-plastic behaviors are considered, the elastic strain increment can be expressed as:

$$\Delta\varepsilon_{kk}^{el} = \Delta\varepsilon_{ij} - \Delta\varepsilon_{ij}^{th} - \Delta\varepsilon_{ij}^{p}, \quad (19)$$

Where $\Delta\varepsilon_{ij}^{p}$ can be obtained according to the backward Euler Integration and plastic constitutive

theory [19] as

$$\Delta\varepsilon_{ij}^{p} = \frac{3S_{ij}^{t+\Delta t}}{2\bar{\sigma}^{t+\Delta t}}\Delta\bar{\varepsilon}^{p}; \tag{20}$$

$$\sigma_{ij}^{t+\Delta t} = \sigma_{ij}^{t} + \Delta\sigma_{ij} \tag{21}$$

Where $S_{ij}^{t+\Delta t}$ are the components of the deviatoric tensor of the Cauchy stress at $t+\Delta t$; $\bar{\sigma}^{t+\Delta t}$ is the Mises stress at $t+\Delta t$, which is dependent on the equivalent plastic strain increment $\Delta\bar{\varepsilon_p}$. After some manipulations, a closed form expression for $\Delta\bar{\varepsilon}^{p}$ can be obtained:

$$\bar{\sigma}^{t+\Delta t} + 3G\Delta\bar{\varepsilon_p} - \bar{\sigma}^{pr(t+\Delta t)} = 0, \tag{22}$$

Where the Mises stress and equivalent plastic strain at $t+\Delta t$ should obey the irradiated strain-hardening curve in Section 2.2.1; $\bar{\sigma}^{pr(t+\Delta t)}$ is the trial Mises stress with the assumption of no plastic strain increments in Eq. (19). Eq. (22) is a nonlinear equation of $\Delta\bar{\varepsilon_p}$. Newton Iteration is applied to solve this nonlinear equation. When the converged equivalent plastic strain increment is obtained, the stress and strain can be updated.

Based on the developed constitutive relations and stress update methods for the fuel meat and cladding, the subroutines UMAT are written to simulate the non-homogeneous irradiation-induced mechanical behaviors.

3. Finite element model

3.1. Finite element geometric model

A dispersion nuclear fuel plate is taken as the research object, whose length and width is much larger than its thickness. The bonding between the fuel meat and the cladding is assumed perfect. As mentioned above, the thermo-mechanical behaviors evolution for un-uniform irradiation conditions is to be simulated. According to the symmetry in geometry and loading, a 1/8 part of the whole fuel plate is set as the finite element geometric model including the corresponding parts of fuel meat and cladding, as illustrated in Fig.1. Using the reduced Integration element C3D8RT, the FE model in Fig.1 is meshed with 49950 elements and 56848 nodes.

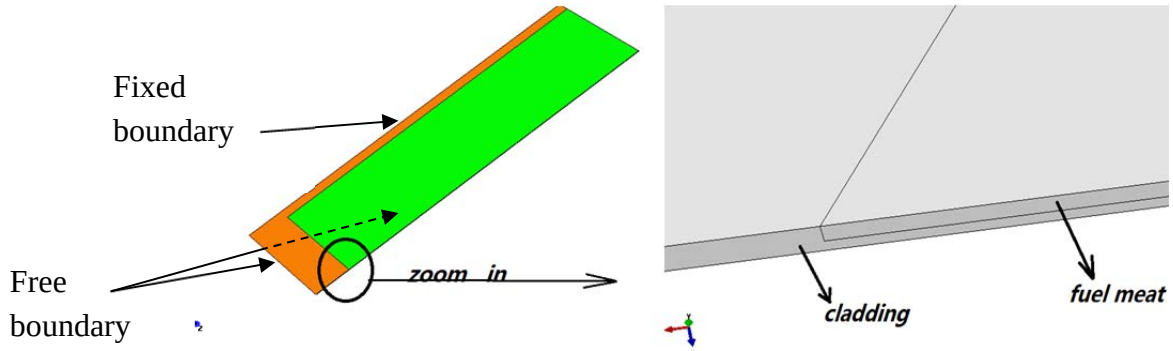

Figure.1 FEM Model

3.2 .boundary conditions

The boundary conditions to determine the temperature field are given as

(1) The surface to contact with the coolant water satisfies the convection boundary condition $-\mathrm{K}\frac{\partial T}{\partial n} = h(T - T_f)$, where the temperature of periphery fluid T_f is 573K. And the used heat transfer coefficient is $2\times10^{-2}\ W/mm^2K$.

(2) Other surfaces satisfy: $-\mathrm{K}\frac{\partial T}{\partial n} = 0$.

The used boundary conditions to determine the mechanical field are as follows
(1) Fixed boundary condition is applied to the side surface, shown as Fig.1
(2) The unseen lower surface and the front surface are set as free boundaries.
(3) Other surfaces are applied with symmetric boundary conditions.

4. Results and discussion

In this section, the effectiveness of the irradiation hardening simulation is validated, and the obtained temperature field and mechanical ones are to be shown and discussed.

4.1. Validation of irradiation hardening simulation

In order to make the correctness of irradiation hardening simulation confirmed, node M in the cladding is selected and the calculated Mises stresses and equivalent elasto-plastic strains at different time have been output. Taking them as the longitudinal and transverse ordinates respectively, three points can be produced in Fig.3. Meanwhile the irradiation hardening curves of the cladding material at the corresponding irradiation damage and temperature are plotted in Fig.3. It can be seen that the obtained computation results obey the irradiation hardening curves, which denotes that the irradiation hardening effect is correctly simulated.

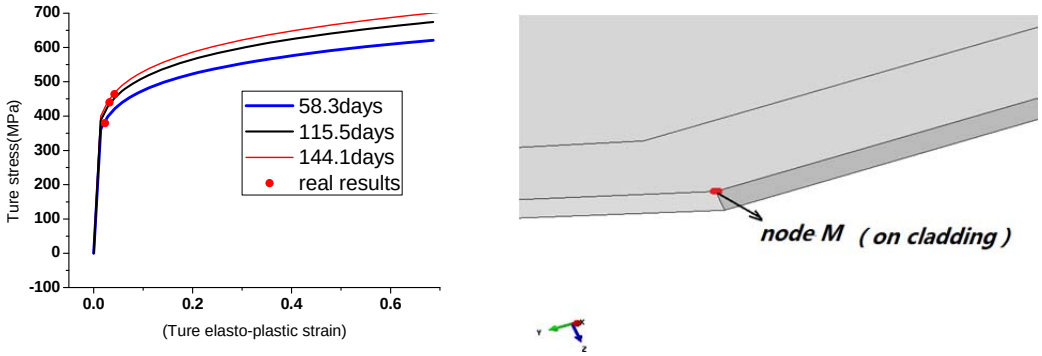

(a) (b)

Figure.2 (a) The stress-strain curves and the numerical results of (b) node M in the cladding

4.2. The temperature results

The calculated temperature field under heterogeneous irradiation condition is depicted in Fig.3 (a). It can be observed that the highest temperature with the red color locates in the fuel meat, precisely speaking, in the middle location along both the length and thickness directions. These phenomena result from the higher heat generation rate there. Thus, two paths in Fig.3 (b) are chosen to output the calculated temperatures at different time. The results under the uniform irradiation condition in Fig.4 are unchanged along the length direction of fuel plate. However, the temperature distribution under non-homogeneous conditions is approximately linear along the two paths, which is closely related to the heat generation rate of fuel meat. From 1.1 days to 144.1 days, the temperature

changes only 0.5 K, it is obvious that the temperature variation with burnup is very slight with a constant irradiation condition. Meanwhile, from comparison of the results along Path 1 and Path 2, it can be found that the maximum temperature in Path 1 is about 9K higher than the one in Path 2, which is for the reason that Path 2 is closer to the coolant water.

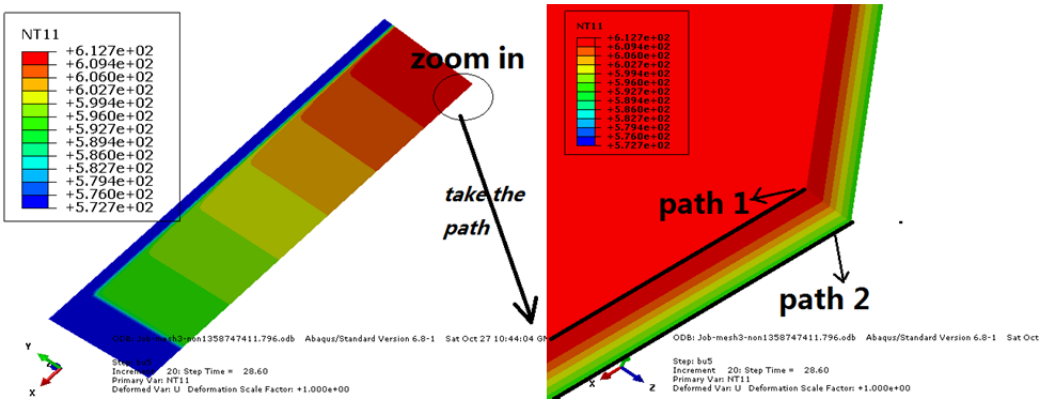

(a) (b)

Figure.3 (a) Temperature distribution at 144.1days and (b) the paths to output the results

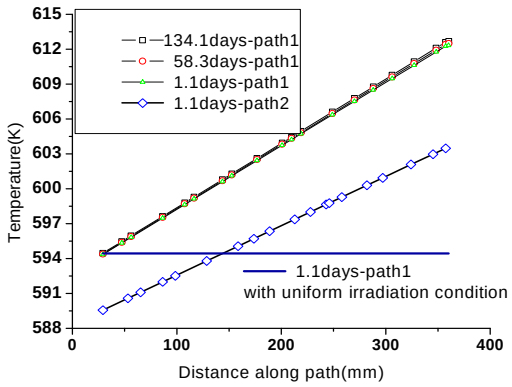

Figure. 4 Temperature distribution in the fuel meat

4.3. Mechanical behaviors in the cladding

The cladding is the first barrier to keep the radioactive substance from leakage. It's of huge importance to maintain its integrity. For the metal material, the Mises stress is firstly concerned. The contour plot at 144.1days is given in Fig.5. One can see that a stress concentration zone exists in the corner of cladding with the largest Mises stress reaching 468.4MPa, which is caused by the fixed boundary condition. To investigate the Mises stress distribution in the zone, two paths were taken in Fig.6. Through comparison of the results on path1 and path2, it can be discovered that path1 has slightly higher Mises stress than path2, as is shown in Fig. 6(a). Also, one can find that with increasing time the Mises stress demonstrate the same variation law on path1 as that the maximum numerical result always appears at the tip of the stress concentration zone. Meanwhile, from 29.7days to 144.1days, the maximum Mises stress on path1 increases from 341.52MPa to 465.4MPa. Observation of Mises stress distribution in the cladding part with the fuel meat

underneath shows that there exist the largest results in the middle location of fuel plate, that is, they locates at the right zone of the finite element model. It is induced by the fact that there exists the largest neutron flux which leads to the highest heat generation and irradiation swelling of fuel meat together with strengthened irradiation hardening in the cladding. This is the result of un-uniform irradiation conditions. In a word, it is necessary to optimize the constraint and irradiation conditions for fuel elements in order to assure their safety.

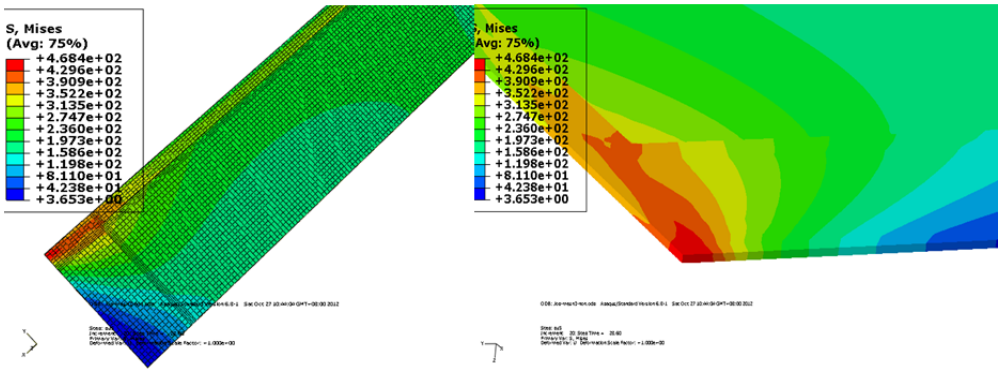

(a) (b)

Figure.5 (a) The Mises stress contours and (b) the stress concentration zone in cladding at 144.1days

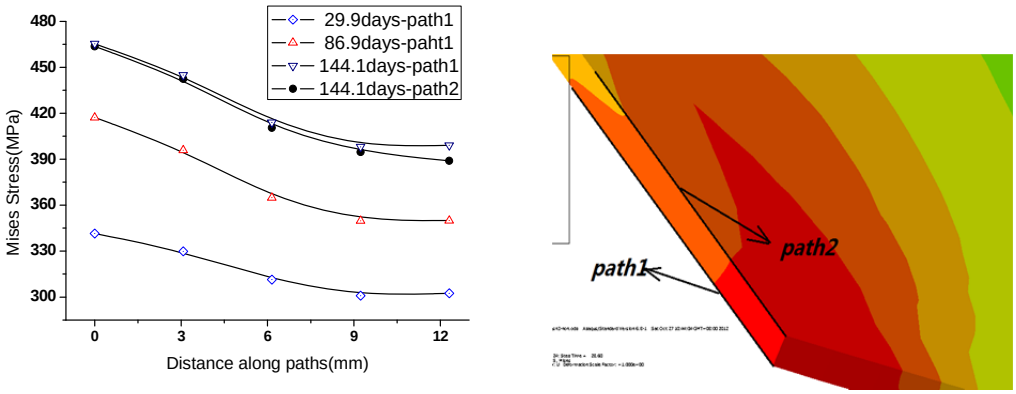

Figure.6 (a) The Mises Stress in different time along (b) the two paths in cladding

4.4. Deformation in the thickness direction

It is well known that the exceeding deformation along the plate thickness direction will narrow the coolant water channel, which will further lead to degradation of the heat transfer coefficient between the fuel plate and the coolant water. This could even result in accident with rapid temperature rise. Thus, the deformation in the thickness direction of fuel plate under nonhomogeneous neutron flux is mainly investigated. Fig.7 (a) reveals the displacements in the thickness direction of fuel plate along the surface path depicted in Fig. 7 (b). It can be observed that (1) the displacements is very small at the part with no fuel meat underneath and they change little with time; (2) the large displacements mainly exist in the part with the fuel meat underneath, and they increase with time distantly; (3) as expected, the maximum deformation arises in the middle part along the plate length direction, and its increasing rate with time is highest. The fuel plate tends to be an arch. As can be easily understood, the main contribution of the above deformation is from

the irradiation swelling of fuel meat, and the swelling is largest in the middle together with the highest temperature there. For the sake of in-pile safety, the initial gap between the fuel elements in the fuel assembly should be properly designed.

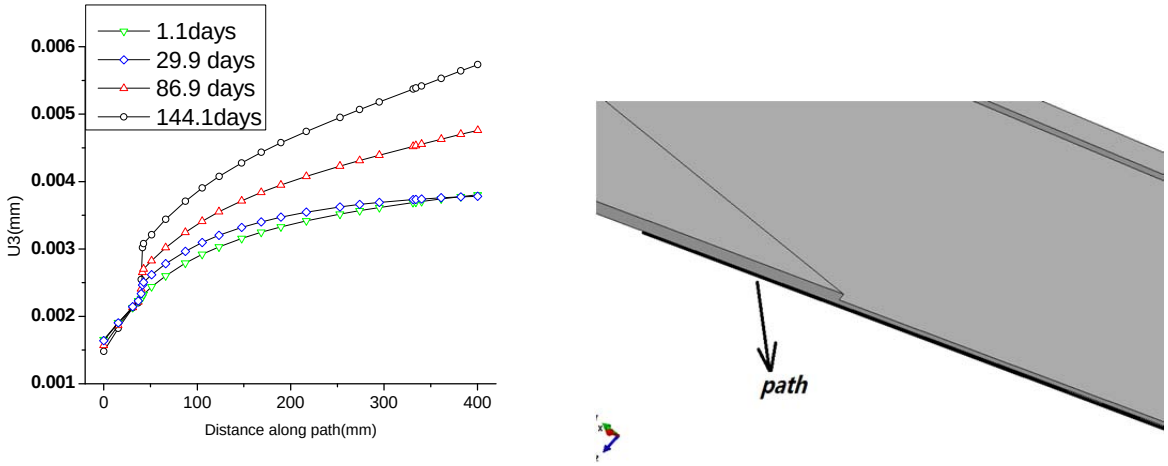

(a) (b)

Figure.7 (a) The displacements in the thickness direction along (b) the plate surface path

5. Conclusions

The stress update algorithms and UMAT subroutines for the dispersion nuclear elements are effective to simulate the thermal-mechanical behaviors under the assumed linearly distributed irradiation condition. Several conclusions can be obtained as the following

(1) The temperature distribution in the equivalent meat is corresponding to the heat generation setting and the middle position holds the highest temperature.

(2) The fixed long side of the cladding causes a stress concentration zone in the fuel plate corner, and the high neutron flux in the middle location leads to existence of the relatively large stress with the fuel meat underneath.

(3) Deformation of the thickness is un-uniformly distributed along the plate length direction and the largest one is at the middle position with the highest neutron flux.

In the future, other irradiation damage effects will be further included in our constitutive relation and numerical simulation, and different constraint conditions and more practical heterogeneous irradiation conditions for dispersion fuel plates will be studied.

Acknowledgement

The authors thank for the supports of the Natural Science Foundation of China (11172068, 91226101, 11272092,11072062, 91026005), the Research Fund for the Doctoral Program of Higher Education of China (20110071110013), Strategic Priority Research Program" of the Chinese Academy of Sciences (Grant No. XDA01020304).

References

[1] A.Leenaers, S. Van Den Berghe, S. Dubois, J. Noirot, M, Ripert, P. Lemoine, Microstructural

Analysis of Irradiated Atomized U(MO) Dispersion Fuel in an Al Matrix with Si Addition, RRFM2008 Transactions, Section2: Fuel Development and Fabrication,pp. 106-110.

[2] H.Taboada.J. Rest, MV. Moscarda, M, Markiewicz, E. Estevez, in: Proceedings of the 24th International Management on Reduced Enichement for Rearch and Test Reactors, San Carlos de Bariloche, Argentina, 3-8 November 2002.

[3] Rest, J., 1995. The DART Dispersion Analysis Research Tool: A Mechanistic Model for Predicting Fission-Product-Induced Swelling of Aluminum Dispersion Fuels, ANL-95/36.

[4] Hayes, S.L., Hofman, G.L., Meyer, M.K., Rest, J., Snelgrove, J.L., 2002. in: 2002 International Meeting on Reduced Enrichment for Research and Test Reactors, Bariloche, Argentina, 3–8 November.

[5] Hayes, S.L., Meyer, M.K., Hofman, G.L., Snelgrove, J.L., Brazener, R.A., 2003. in: Proceedings of the 2003 International Meeting on Reduced Enrichment for Research and Test Reactors, Chicago, IL, 5–10 October.

[6] Marelle, V., Dubois, S., Ripert, M., Noirot, J., Lemoine, P., 2007. in: The RERTR-2007 International Meeting on Reduced Enrichment for Research and Test Reactors, 23–27 September, Diplomat Hotel – Prague, Prague, Czech Republic.

[7] Marelle, V., Huet, F., Lemoine, P., 2004. in: Proceedings of the Eighth International Topical Meeting on Research Reactor Fuel Management, München, Germany, 21–24 March.

[8] Saliba, R., Taboada, H., Moscarda, M.V., 2003. in: 2003 International Meeting on Reduced Enrichment for Research and Test Reactors, Chicago, IL, 5–10 October.

[9] Lee Van Duyn, 2003. Evaluation of the Mechanical Behavior of a Metal-matrix Dispersion Fuel for Plutonium Burning, Georgia Institute of Technology: A Thesis for the Degree Master of Science in Mechanical Engineering.

[10] Shurong Ding, Xin Jing, Yongzhong Hou, Lin and Li, Journal of Nuclear Materials 374(2008)453-460.

[11] Shurong Ding, Yongzhong Huo, XiaoQing Yan, Journal of Nuclear Materials (2009), doi:10.1016/j.jnucmat. 2009.04.015.

[12] Qiming Wang, Xiaoqing Yan, Yongzhong Huo, Shurong Ding, Mechanical behaviors of the dispersion nuclear fuel plates induced by fuel particle swelling and thermal effect I: effects of variations of the fuel particle volume fractions, *Journal of Nuclear Materials*, Vol. 400, No. 2, May 2010, pp. 157-174..

[13] N.Okubo,Y. Miwa, K. Kondo,Y. Kaji, J. Nucl. Mater. 386-388(2009)290-293.

[14] Aboudi J., Mechanics of composite materials[M, Elsevier, Amsterdam, 1991.

[15] Aboudi J., Micromechanical analysis of composites by the method of cells-update[J]. Appl. Mech. Rev., 1996,49: S83-S91.

[16] J.C.Maxwell, A Treatise on Electricity and Magnetism[M]. Oxford: Clarendon Press, 1873.

[17] Mori T., Tanaka K., Average stress in matrix and average elastic energy of materials with misfitting inclusions[j]. Acta Matal, 1973, 21: 571-574.

[18] D.L.Hagman.G.A Reyman.MATPR-Verson11, A Handbook of Materials Properties for use in the Analysis of Light Water Reactor Fuel Rod Behavior, NUREG/CR-0497, TREE-1280,Rev, vol,3,1979..

[19] Belytschko, T., Liu, W.K., Moran, B.,2000. Nonlinear Finite Elements for Continua and Structures, John Wiley & Sons Ltd., U.K.